

Morpholino-mediated Knockdown of *DUX4* Toward Facioscapulohumeral Muscular Dystrophy Therapeutics

Jennifer CJ Chen^{1,2}, Oliver D King^{1,2}, Yuanfan Zhang^{3,4}, Nicholas P Clayton⁵, Carrie Spencer^{1,2}, Bruce M Wentworth^{5,6}, Charles P Emerson, Jr^{1,2} and Kathryn R Wagner^{3,4,7,8}

¹Department of Cell and Developmental Biology, University of Massachusetts Medical School, Worcester, Massachusetts, USA; ²Department of Neurology, University of Massachusetts Medical School, Worcester, Massachusetts, USA; ³The Hugo W. Moser Research Institute, Kennedy Krieger, Baltimore, Maryland, USA; ⁴Graduate Program in Cellular and Molecular Medicine, The Johns Hopkins School of Medicine, Baltimore, Maryland, USA; ⁵Sanofi Genzyme, Cambridge, Massachusetts, USA; ⁶Current address: Department of Biology, Sarepta Therapeutics, Cambridge, Massachusetts, USA; ⁷Department of Neurology, The Johns Hopkins School of Medicine, Baltimore, Maryland, USA; ⁸Department of Neuroscience, The Johns Hopkins School of Medicine, Baltimore, Maryland, USA.

Derepression of *DUX4* in skeletal muscle has emerged as a likely cause of pathology in facioscapulohumeral muscular dystrophy (FSHD). Here we report on the use of antisense phosphorodiamidate morpholino oligonucleotides to suppress *DUX4* expression and function in FSHD myotubes and xenografts. The most effective was phosphorodiamidate morpholino oligonucleotide FM10, which targets the polyadenylation signal of *DUX4*. FM10 had no significant cell toxicity, and RNA-seq analyses of FSHD and control myotubes revealed that FM10 down-regulated many transcriptional targets of *DUX4*, without overt off-target effects. Electroporation of FM10 into FSHD patient muscle xenografts in mice also down-regulated *DUX4* and *DUX4* targets. These findings demonstrate the potential of antisense phosphorodiamidate morpholino oligonucleotides as an FSHD therapeutic option.

Received 22 March 2016; accepted 18 May 2016; advance online publication 5 July 2016. doi:10.1038/mt.2016.111

INTRODUCTION

Facioscapulohumeral muscular dystrophy (FSHD)1 and 2 are genetic diseases whose primary manifestations are weakness and wasting of muscles of the face, shoulder girdle, and upper arms. FSHD1, representing ~95% of cases, is associated with deletions of macrosatellite D4Z4 repeats in the subtelomeric region of chromosome 4q35, leaving 1–10 D4Z4 repeats.¹ FSHD2 is in most cases associated with mutations in *Structural Maintenance Of Chromosomes Flexible Hinge Domain Containing 1* (*SMCHD1*) on chromosome 18 (ref. 2). Both of these mutations lead to relaxation of chromatin at the 4q35 D4Z4 repeat array, allowing aberrant transcription in muscle of a full-length form of *DUX4* mRNA (*DUX4-fl*), which encodes a double homeobox transcription factor.^{2–6} Development of laboratory animal models of FSHD have been challenging, due in part to the unknown pathophysiologic mechanism of *DUX4* action and the restricted emergence of the D4Z4-*DUX4* chromosomal architecture in primates and

Afrotheria.^{7,8} Nevertheless, the evidence that *DUX4* is an FSHD disease gene is compelling, including the findings that: (i) both FSHD1 and 2 are associated with particular “permissive” 4q35A haplotypes that include a polyadenylation signal required for production of stable *DUX4-fl* mRNA from the telomeric D4Z4 repeat; (ii) overexpression of *DUX4-fl* induces a large cohort of germline genes that are also up-regulated in FSHD muscle^{5,9,10}; and (iii) overexpression of full-length *DUX4* protein is toxic in muscle, both *in vitro* and *in vivo*.^{11,12}

These findings identify *DUX4* as a promising therapeutic target for antisense therapy. Antisense oligonucleotides are being developed as therapeutics for other neuromuscular diseases including Duchenne muscular dystrophy, spinal muscular atrophy (SMA) and myotonic dystrophy.^{13–16} Here we report a proof-of-concept study of the therapeutic potential of antisense phosphorodiamidate morpholino oligonucleotides (PMOs) for the treatment of FSHD, by targeting *DUX4* and demonstrating efficacy in both FSHD myogenic cells and human muscle xenografts.

RESULTS

Transcriptome sequencing (RNA-seq) was performed on cultured myotubes derived from the biceps of 6 FSHD subjects and their unaffected first-degree relatives to establish a reference transcriptional signature (detailed later in this section). Consistent with previous studies,¹⁰ FSHD myotubes expressed elevated levels of direct and indirect transcriptional targets of *DUX4* (ref. 9). The mRNA levels of *DUX4* targets serve as biomarkers of *DUX4* activity, and can be more readily quantified than levels of *DUX4* mRNA or *DUX4* protein, which are often quite low (ref. 9 and Materials and Methods).

PMOs that target the *DUX4-fl* transcript (**Figure 1a** and **Supplementary Table S1**) were tested for their ability to suppress the expression of *DUX4* protein and selected *DUX4* target genes.^{17–19} Differentiating myotube cultures derived from FSHD subjects were treated for 4 days with control or *DUX4* PMOs, and then analyzed for biomarker expression to assay knockdown efficiency. FM10 and, to a lesser extent, FM9 had the greatest effects,

The first three authors and the last two authors contributed equally to this work.
Correspondence: Kathryn R Wagner (wagnerk@kennedykrieger.org)

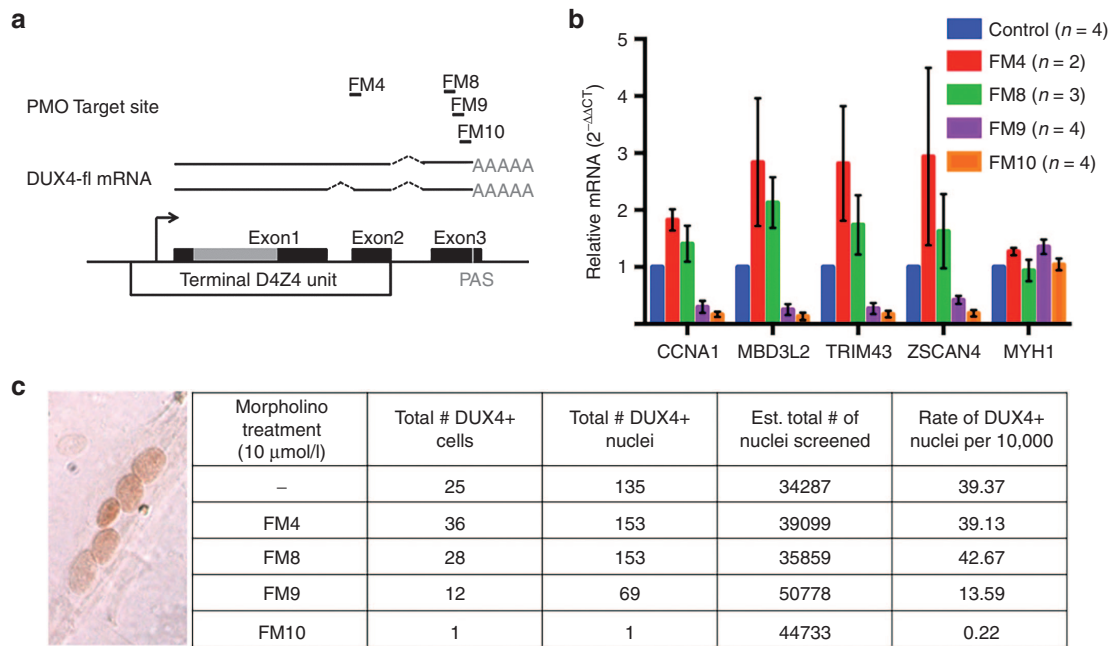


Figure 1 DUX4 and DUX4 target gene knockdown in facioscapulohumeral muscular dystrophy (FSHD) myotubes *in vitro*. **(a)** Schematic demonstrating *DUX4-fl* transcript and relative targets of phosphorodiamidate morpholino oligonucleotides (PMOs); PAS, polyadenylation signal. **(b)** FSHD biomarker expression analysis of 4-day FSHD myotube cultures treated with standard control or *DUX4*-targeting morpholinos. Significant decreases in *CCNA1*, *MBD3L2*, *TRIM43*, and *ZSCAN4* biomarker expression were observed in myotube cultures treated with 10 μmol/l FM10 (**P*-value < 0.05, Student's *t*-test performed on Δ Cts normalized to *RPL13A*); an intermediate effect was observed in FM9-treated cultures. *MYH1* expression was not affected by PMO treatment. Data are presented as the mean fold change \pm standard error of mean (SEM) relative to standard control morpholino. **(c)** DUX4 protein expression analysis of 4-day FSHD myotube cultures treated with standard control or *DUX4*-targeting morpholinos. DUX4 protein was detected by immunostaining with C-terminal DUX4-specific P4H2 antibody. The greatest decrease in DUX4-positive nuclei was observed in myotube cultures treated with 10 μmol/l FM10; an intermediate effect was observed in FM9-treated cultures.

consistently decreasing levels of DUX4 target genes *ZSCAN4*, *MBD3L2*, and *TRIM43* (Figure 1b and Supplementary Figure S1), establishing that these compounds block DUX4 function. Notably, FM10 targets the same 25-nucleotide sequence as PMO-PAS, one of two PMOs (of five tested) that showed highest efficacy in knocking down *DUX4* expression in a recent independent study by Marsollier *et al.*²⁰ Both FM10 and FM9 target the polyadenylation signal region of the *DUX4* transcript. The other PMOs tested in this series, which target regions 5' of those two, did not decrease biomarker expression. None of the PMOs disrupted expression of *myosin heavy chain 1*, a marker of myogenic cell differentiation (Fig. 1 and Supplementary Figure S1). FM10 down-regulation of DUX4 target genes in FSHD cells was dose-dependent, with ED₅₀ (the dose required to achieve 50% of FSHD biomarker knockdown) in the range 1–3 μmol/l, and maximal response between 10–20 μmol/l (see Supplementary Figure S2). Cell viability assays performed on FSHD cells treated with FM10 morpholinos conjugated to a cell penetrating peptide, Peptide B (PPMO;²¹), revealed no toxicity at concentrations up to 500 μmol/l (see Supplementary Figure S3).

PMO effects on protein levels of DUX4 were evaluated in control and *DUX4* PMO-treated FSHD myotube cultures by immunostaining with an antibody targeting a C-terminal region in the full-length DUX4 protein that is absent from the alternatively spliced “short” DUX4, which is not thought to be a toxic protein.⁵ DUX4-positive nuclei were reduced in FM9-treated myotubes and almost undetectable in FM10-treated myotubes (Figure 1c), establishing their inhibition of DUX4 protein expression.

Transcriptomes of FSHD and control myotube cultures treated with FM10 or standard control PMO were determined by RNA-seq. *P*-value < 10⁻⁴ was used as the cutoff for significance in tests of differential expression. In myotube cultures from two FSHD subjects, 47 genes differed significantly between FM10 versus control PMO treatment, with an associated false discovery rate of 0.066 (Figure 2b and Supplementary Table S2). Of these 47 genes, 46 had lower expression with FM10 treatment than with control PMO.

To assess whether these changes reflected a suppression of FSHD-associated transcription, we compared PMO transcriptome results to the RNA-seq data from myotubes of six FSHD subjects versus their unaffected relatives, in which 121 genes were significantly upregulated in FSHD and four were significantly downregulated (false discovery rate = 0.021; Figure 2a and Supplementary Table S3), and to the 213 DUX4 targets from Supplementary Table S1 of Yao *et al.*,¹⁰ which includes 94 of the 121 genes significantly upregulated in FSHD versus unaffected myotubes. Both false positives and false negatives have a stochastic component (including sampling error), which limits how well sets of significantly altered genes from different studies will agree, even for identically designed and equally powered studies (which these are not). As a more relaxed measure of agreement, though still subject to sampling error, we checked whether the significantly altered genes in one study were changed in a consistent direction in the other study, regardless of significance. About 89% of the genes that were significantly reduced with FM10 had at least

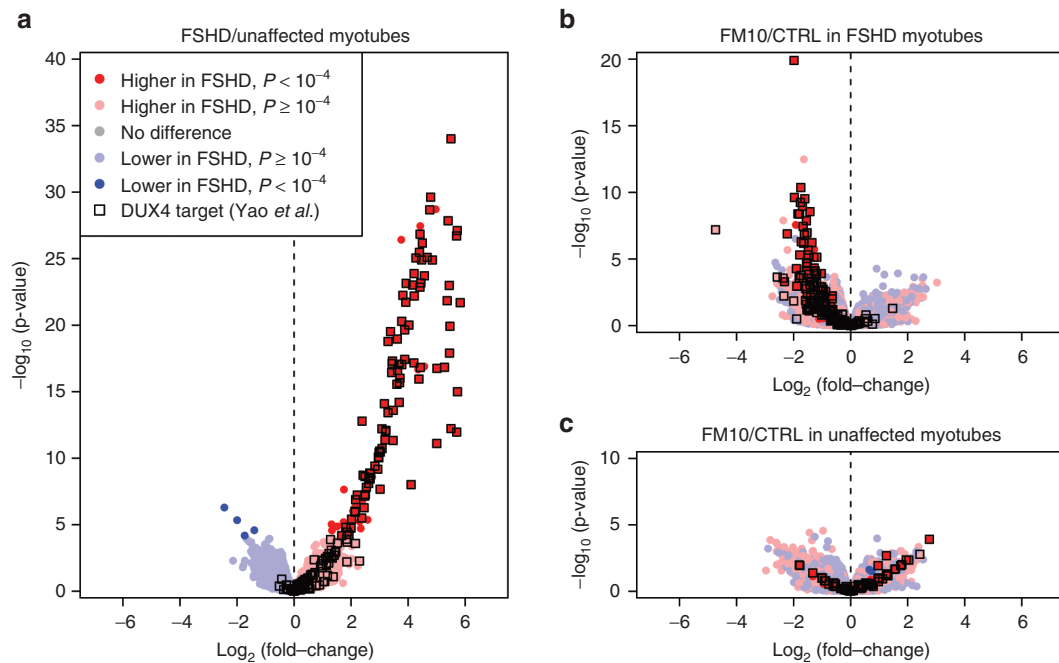


Figure 2 RNA-seq analysis of facioscapulohumeral muscular dystrophy (FSHD) versus unaffected myotube cultures and FM10 versus control phosphorodiamidate morpholino oligonucleotide (PMO)-treated myotube cultures. These volcano plots show $\log_2(\text{fold-change})$ versus $-\log_{10}(P\text{-value})$ for tests of differential expression of $\sim 37,000$ genes detected by RNA-seq, for three comparisons: **(a)** myotube cultures from FSHD subjects versus unaffected first-degree relatives ($n = 6$ pairs); **(b)** FM10 versus control (CTRL) PMO-treated myotube cultures from FSHD subjects ($n = 2$); and **(c)** FM10 versus control (CTRL) PMO-treated myotube cultures from unaffected subjects ($n = 2$). The two subjects in **b** are first-degree relatives of the two subjects in **c**, and are unrelated to the 12 subjects in **a**. To aid in comparisons between plots, the color-coding of points in all plots is determined by direction and significance of changes in **a**: genes whose expression is higher in FSHD than control myotubes are colored red if $P\text{-value} < 10^{-4}$ and pink otherwise; genes whose expression is lower in FSHD than control myotubes are colored blue if $P\text{-value} < 10^{-4}$ and light blue otherwise. In all plots, black squares are overlaid on the DUX4 targets from Table S1 of Yao *et al.*¹⁰ Of the 46 genes that were significantly decreased by FM10 in **b**, 41 had elevated expression in FSHD versus control myotubes in **a**, significantly so for 32; and 30 were among the DUX4 targets from Table S1 of Yao *et al.*¹⁰ Conversely, 116 of the 121 genes that were significantly elevated in FSHD versus unaffected myotubes in **a**, and 162 of the 185 detected DUX4 target genes from Table S1 of Yao *et al.*¹⁰ had at least some reduction by FM10 in **b**. $P\text{-values}$ are from likelihood-ratio tests for negative binomial regression (R package edgeR), and prior counts of 1 were used to avoid infinite log fold-changes; see Materials and Methods for details.

some upregulation in FSHD myotubes, and conversely 96% of the genes that were significantly upregulated in FSHD myotubes had at least some reduction with FM10 (**Figure 2a,b**). The reduction was not typically to the level of DUX4 targets observed in control cells: many DUX4 targets were elevated more than 16-fold in FSHD versus unaffected myotubes (\log_2 fold-change > 4 in **Figure 2a**), whereas few showed more than four-fold decrease by FM10 versus control PMO (\log_2 fold-change < -2 in **Figure 2b**), and this is not because the two FM10-treated FSHD samples had particularly low levels of the DUX4 targets pretreatment (see **Supplementary Figure S4**).

RNA-seq analysis of FM10 myotube cultures from the two unaffected first-degree relatives provides another view of off-target effects, unclouded by DUX4 target genes, as unaffected cells express little if any *DUX4-fl*. For these cells, only three genes differed significantly between FM10 and the control PMO ($P\text{-value} < 10^{-4}$), and this is roughly what one expects by chance when testing $\sim 37,000$ genes for differential expression, even if the null hypotheses of equal expression are all true (**Figure 2c**). No genes had $P\text{-value} < 10^{-5}$ or false discovery rate < 0.72 . Thus we observed no clear off-target effects of FM10 based on these samples.

We evaluated FM10 PMO knockdown of *DUX4-fl* in human muscle *in vivo* using an FSHD xenograft model created by

transplanting FSHD affected donor muscle into the hindlimbs of *NOD-Rag1^{null}IL2r γ ^{null}* immunodeficient mice.²² Engrafted muscle from FSHD biopsy donors and FSHD autopsy donors regenerated and was revascularized and reinnervated by 4 months post-transplant. Importantly, *DUX4-fl* as well as DUX4 target gene expression in these xenografts has been shown to mirror those of the donor muscle tissue.²² FM10 or standard control PMO was electroporated into FSHD xenografts, and mice were analyzed after 2 weeks (**Figure 3a**). Human xenografts were confirmed by immunohistochemistry using antihuman spectrin and antihuman lamin a/c antibodies to stain specifically for human muscle fiber membranes and human nuclei, respectively (**Figure 3b**). In FSHD xenografts, FM10 reduced *DUX4-fl* expression to nearly undetectable levels compared with control PMO (**Figure 3c**). FM10 treatment also reduced the expression of DUX4 target genes *MBD3L5* and *ZSCAN4* in xenografts compared with control PMO (**Figure 3d**).

DISCUSSION

Our study provides proof-of-concept that antisense PMO targeted specifically to the essential *DUX4* polyadenylation signal can significantly diminish the expression of *DUX4-fl* and DUX4 target genes that serve as biomarkers of DUX4 activity,^{5,23,24} both *in vitro*

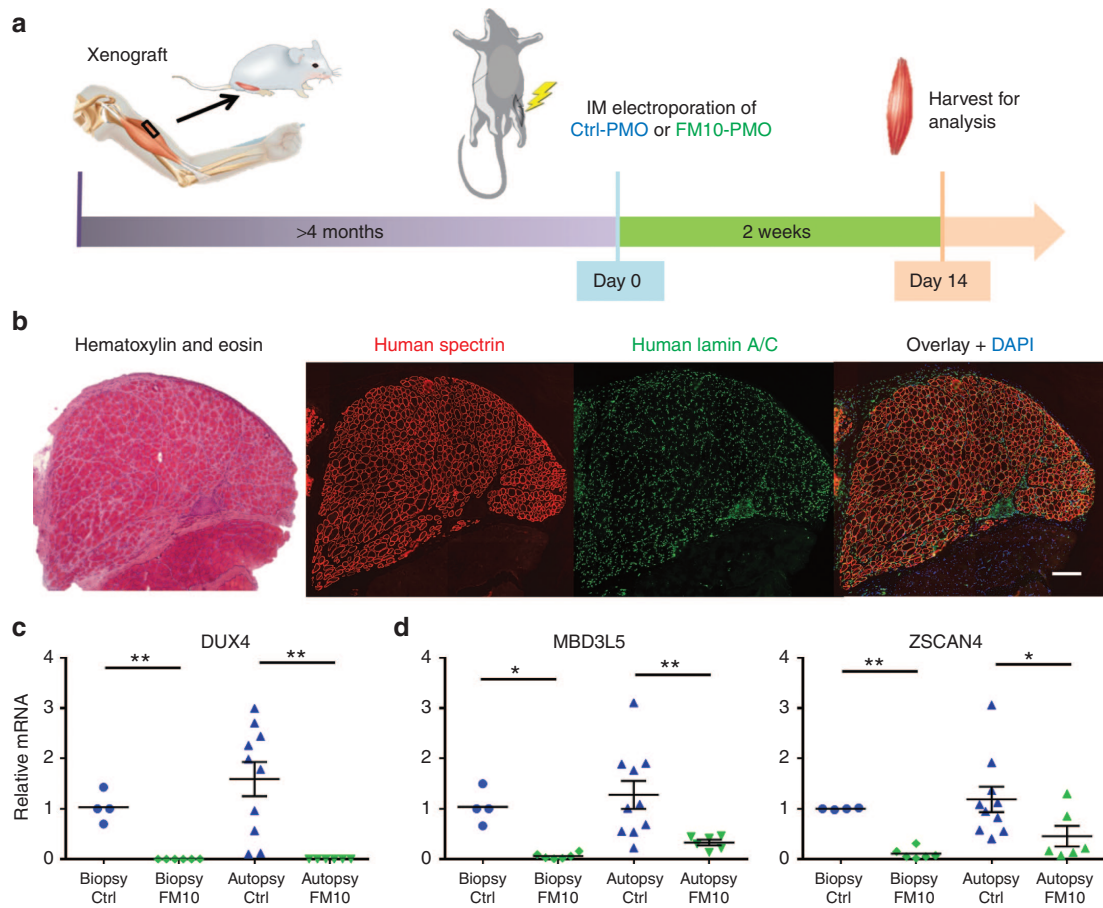


Figure 3 *In vivo* validation of FM10 knockdown of *DUX4-fl* and *DUX4* target genes in a human facioscapulohumeral muscular dystrophy (FSHD) xenograft model. **(a)** Schematic of the *in vivo* study design. FSHD patient muscle was transplanted into the *tibialis anterior* space of NRG mice. Xenografts fully regenerated in the mouse leg for more than 4 months, were treated with Control- or FM10- phosphorodiamidate morpholino oligonucleotides (PMO) via electroporation, and harvested after 2 weeks. **(b)** Histology of a four-month FSHD xenograft. Immunohistochemistry of the human-specific muscle membrane protein spectrin and nuclear envelope protein lamin A/C confirmed that the xenograft was well regenerated. Human spectrin (red), human lamin A/C (green), DAPI (blue). Scale bar: 200 μ m. **(c)** Expression analysis of *DUX4-fl* and **(d)** of *DUX4* target genes *MBD3L5* and *ZSCAN4* in xenografts from biopsy and autopsy donor groups, all with FSHD, treated with Control- and FM10-PMOs. Statistical tests were performed on Δ Cts, normalized to housekeeping genes *PPIA* and *GUSB*. Significant decreases were observed for all three genes with FM10 treatment (** $P < 0.01$; * $P < 0.05$, all tests two-tailed). No correlation was detected between housekeeping gene expression and treatment. The biopsy group consisted of xenografts from three FSHD donors ($n = 4$ Ctrl; $n = 6$ FM10); to address between-donor rather than within-donor variance in response to FM10, Δ Cts for xenografts from each donor were averaged, and a paired *t*-test performed on the per-donor averages. All xenografts in the autopsy group were from a single FSHD donor ($n = 10$ Ctrl; $n = 6$ FM10), and an unequal variance *t*-test was used for this data. Expression levels for each xenograft are shown as fold-changes relative to the per-donor mean Δ Ct for the Ctrl PMO ($2^{-\Delta\Delta Ct}$), with mean of the per-donor averages (biopsy) or mean \pm standard error of mean (SEM) (autopsy) also indicated.

and in human xenografted muscle *in vivo*. Previously, PMOs and other antisense oligonucleotides targeting 3' elements of *DUX4-fl*, including splice acceptor sites 2 and 3 and the polyadenylation signal, have been shown to reduce expression of *DUX4* and select *DUX4* targets *in vitro*.^{20,25} Our *in vitro* studies provide a global view of transcriptional changes associated with *DUX4* knock-down, and provide experimental data on off-target effects that complement *in silico* predictions. In particular, the 25-nucleotide sequence targeted by FM10 is the same as that targeted by PMO-PAS in Marsollier *et al.*, which did not have strong off-target candidates based on a Basic Local Alignment Search Tool (BLAST) search and predictions of binding energies.²⁰ Differences in dose response results observed here and by Marsollier *et al.* are likely due to use of different timing and methods of PMO delivery: Marsollier *et al.* transfected leish-PMO cationic complexes at day

2 of differentiation²⁰; in our hands, we found that lipid transfection was quite toxic to our cells (data not shown), and therefore elected to simply treat cells with naked PMO without lipid starting at day 0 of differentiation.

Our studies of FM10 PMO also evaluate its cell toxicity and *in vivo* effect on *DUX4*, which are essential in pursuing therapeutic development. Future studies will be needed to evaluate the efficacy of repeated and systemic administration of PMOs in knocking down *DUX4* target gene expression, and although the pathophysiology of FSHD remains incompletely understood, we anticipate that one or more of these *DUX4* target genes is responsible for FSHD muscle weakness and could serve as a direct therapeutic target. Our findings, therefore, provide comprehensive evidence that antisense PMO technology is a potential therapeutic option for FSHD.

MATERIALS AND METHODS

Human subjects, genotyping, and biopsy. This study was approved by the Johns Hopkins School of Medicine Institutional Review Board. The Declaration of Helsinki Protocols was followed, and written informed consent was received from participants prior to inclusion in the study. Subjects with FSHD and their first degree unaffected relatives were recruited and screened for biomaterial contributions. FSHD status was determined by pulsed field electrophoresis and southern blotting of leukocyte DNA by Dr. Steven A. Moore and the University of Iowa Diagnostic Laboratories, Iowa City, IA, and included identification of the EcoRI/BlnI 4q35 D4Z4 repeat length with a p13E11 probe, and 4qA/4qB allele typing of HindIII fragments.^{26–29} Subjects with a positive FSHD diagnosis were categorized with an A, B or C designation, and unaffected control subjects with a confirmed negative genotype were categorized with a U, V, or W designation. Open muscle biopsy was performed on biceps from living donors and deltoid muscle was harvested from autopsy.³⁰ Clinical data for subjects 33A, 33U, 41A, 58A, 61A, and 61B are presented in **Supplementary Table S4**; data for remaining subjects were published previously.^{30,31}

Morpholinos. PMOs were synthesized by Gene Tools, LLC (Philomath, OR), with a 5' primary amine modification to facilitate conjugation with a cell penetrating peptide (CPP) Peptide B²¹; PMOs conjugated to Peptide B are abbreviated as PPMOs. Sequences of PMOs are shown in **Supplementary Table S1**.

Cell culture and in vitro morpholino treatment. Primary muscle cells from FSHD subjects 03A, 13B, 14A, 15A, 15B, 16A, 17A, 18A, 21A, 33A, 41A and first-degree, unaffected relatives 03U, 13U, 14W, 16U, 21U, and 33U were cultured as previously described.³² To assess PMO activity, cells were cultured until >95% confluent, rinsed briefly with PBS (Cellgro Mediatech, Massasas, VA), and then differentiated in Opti-MEM (Invitrogen, Carlsbad, CA) supplemented with 10 $\mu\text{mol/l}$ DUX4-targeting PMO or standard control PMO (Gene Tools, LLC). The standard control PMO designed by Gene Tools, LLC targets a human beta-globin intron mutation that causes beta-thalassemia, and this target is restricted to beta-thalassaemic hematopoietic cells (www.gene-tools.com). Cells were treated with PMOs for 4 days without a medium change, and then harvested for quantitative real-time PCR (qPCR) analysis or immunocytochemistry. To identify ED₅₀ of FM10, cells were cultured as above and treated with 0–15 $\mu\text{mol/l}$ standard control or FM10 PMO for 4 days and assayed for qPCR analysis. Toxicity was assessed with 17A primary muscle cells treated with 0–500 $\mu\text{mol/l}$ standard control or FM10 PPMOs conjugated to CPP Peptide B²¹ in triplicate, using the Celltiter-Glo Luminescent Viability Assay (Promega, Madison, WI) according to manufacturer's instructions. Fluorescence was measured using a Tecan Safire II plate reader operated by Xfluo4 Software v4.51.

Antibodies and immunostaining. Myotube cultures treated with DUX4-targeting PMOs or standard control PMOs were fixed with 4% formaldehyde, pH 7.4 (EMD, Billerica, MA) and immunostained with C-terminal specific mouse-anti-DUX4 clone P4H2 (kindly provided by Drs. Stephen Tapscott and Linda Geng) as previously described.³¹ Secondary detection was performed using the ABC Elite kit (Vector Labs, Burlingame, CA) and 3,3'-diaminobenzidine (DAB) peroxidase staining. DUX4-positive nuclei were counted using DIC microscopy, and total number of nuclei was estimated by counting 10 random fields and multiplying by a factor accounting for area screened. Muscle cryosections (10 μm) were fixed in ice-cold methanol (Thermo Fisher Scientific, Waltham, MA), blocked with anti-mouse IgG (MKB-2213, Vector Labs) for 2 hours, incubated in the primary antibodies for 1 hour (antihuman spectrin (NCL-SPEC1, Leica, Wetzlar, Germany, 1:50) and antihuman lamin A/C (Ab40567, AbCam, Cambridge, UK, 1:200)), followed by 45 minute incubation with secondary antibodies (AlexaFluor 488 goat antimouse IgG1, AlexaFluor 594 goat antimouse IgG2b (Invitrogen, Carlsbad, CA, 1:500)) at room temperature. All nuclei were labeled with 4',6-diamidino-2-phenylindole (DAPI) in mounting medium (P36930, Invitrogen).

RNA isolation, cDNA synthesis, and qPCR analyses. RNA was isolated from cells or xenografts as previously described.^{4,5} cDNA was synthesized using Oligo (dT)₁₆ and Superscript III reverse transcriptase (Invitrogen). Primers were synthesized by Integrated DNA Technologies, Coralville, IA. Primer sequences are listed in **Supplementary Table S5**. Cell qPCR reactions were set up in triplicate using iQ SYBR Green Supermix (Bio-Rad, Hercules, CA) and amplified on a CFX96 Touch Real-time PCR Detection System (Bio-Rad). Results were analyzed using CFX Manager Software, and visualized graphically using Microsoft Excel and Graphpad Prism 6. Expression was normalized to *RPL13A*, which was found to not change significantly in response to any PMO or PPMO treatment. From the xenografts, *DUX4-fl* expression was determined using 100 ng of poly(A)⁺ cDNA by qPCR as described previously.³³ qPCR reactions were performed using Taqman Master Mix (Bio-Rad) with specific Taqman assays for *ZSCAN4* (Hs00537549_m1, Life Tech, Carlsbad, CA), *MBD3L5* (Hs04190573_mH, Life Tech), *GUSB* (Hs99999908_m1, Life Tech) and *PPIA* (Hs99999904_m1, Life Tech) and run on a CFX PCR machine (Bio-Rad). Reactions were set up in duplicate. Statistical tests were performed on ΔCt s, normalized to the mean Ct of *PPIA* and *GUSB*. The samples where *DUX4* was not detected were given a Ct of 45 (total cycle number). The control PMO-treated biopsy group included two 58A, one 61A and one 61B xenograft, and the FM10-PMO biopsy group included three 58A, one 61A, and two 61B xenografts. To address between-donor rather than within-donor variance in response to FM10, multiple xenografts from the same donor in each treatment were averaged at the ΔCt level, then these average levels were used in the paired *t*-tests of control PMO versus FM10. Autopsy xenografts ($n = 10$ Ctrl and $n = 6$ FM10) were from a single donor, and were analyzed with a two tailed *t*-test, assuming unequal variance.

RNA sequencing and analysis. High throughput TruSeq stranded mRNA sequencing (RNA-seq, 50- or 51-bp paired end) was performed by Expression Analysis, Morrisville, NC. To identify differences between FSHD and unaffected muscle cells, sequencing was performed on 4-day differentiated myotube cells from FSHD subjects 03A, 13B, 14A, 16A, 21A, and 33A; and their first-degree, unaffected relatives 03U, 13U, 14W, 16U, 21U, and 33U (respectively). To identify effects of FM10 PMO treatment (both DUX4-dependent and off-target effects), 4-day myotubes from FSHD subjects 15A and 17A, and first degree, unaffected relatives, 15V and 17U (respectively), treated with FM10, standard-control morpholino, or Opti-MEM medium alone were sequenced. Samples from 17A and 17U were treated and sequenced in duplicate, which allows estimation of within-subject variance in response to treatment, but the statistical tests reported here depend on between-subject variance in response to treatments, and use just the first replicate so that all subjects are treated uniformly (Data from both replicates is shown in **Supplementary Figure S4**). FASTQ files of raw RNA-seq reads were mapped to Ensembl human GRCh37 reference genome and transcript annotations (version 7.5) from Illumina iGenomes using TopHat2 (2.1.0)³⁴ and Bowtie2 (2.2.6)³⁵ with options -r 70 -mate-std-dev 40 for the FSHD versus unaffected data and -r 60 -mate-std-dev 40 for the PMO data (which was done later and had a bit shorter average insert length). Counts of reads mapping unambiguously to ~63,000 annotated genes were computed using htseq-count (HTSeq-0.6.1p1, strand-specific mode),³⁶ and imported into R for tests of differential expression using the package edgeR (3.12).³⁷ Total per-sample counts of these reads ranged 74–113 million for the FSHD versus unaffected data, and 63–72 million for the PMO data. Normalization factors for each sample were computed in edgeR with the trimmed mean of M-values normalization method, and used as offsets when modeling the data with negative binomial distributions with the function glmFit. The dispersion parameters were computed with the estimateGLMTagwiseDisp function, shrinking the per-gene estimates toward trended dispersion estimates, with prior degrees of freedom set to 5. Likelihood-ratio tests for differential expression were performed with the function glmLRT. The model formula for the FSHD versus unaffected comparison was $\sim 0 + \text{diseaseGroup} + \text{family}$, and the model formula for

the PMO comparisons was $\sim 0 + \text{diseaseGroup:treatment} + \text{subject}$. Here the diseaseGroup factor has levels FSHD and unaffected, the treatment factor has levels FM10, control, and Opti-MEM, while the family factor and subject factor account for the pairings between first-degree relatives and between multiple treatments of subjects, respectively. To make the coefficients identifiable, the sum of the coefficients for family was constrained to be zero in the first model, as were the sums of the coefficients for FSHD and unaffected subjects in the second model. The three treatments were modeled jointly to allow for shared estimates of dispersion parameters. Results for Opti-MEM were generally similar to the standard control PMO (e.g., **Supplementary Figure S4**). All subjects in the FSHD versus unaffected study were female except for 14A and 14W, which were male; thus an additive effect for sex can be absorbed into the family factor, so it is not used. All subjects in the PMO study were male, except from 15V; as there is just one female sample we did not attempt to adjust for sex, but do note that the gene with the most significant change for FM10 in unaffected samples was XIST, which is expressed from inactivated X-chromosomes; this may be due to the negative-binomial model being a particularly poor fit for this gene, whose read count was $>10,000$ -fold higher for the female unaffected subject than for the male unaffected subject, as the direction of change with FM10 was not consistent in the two subjects. In **Figure 2**, **Supplementary Table S3** and **Supplementary Figure S4** a prior count of 1 was used in computing the $\log_2(\text{counts per million})$ and $\log_2(\text{fold-changes})$, to avoid infinite values; this does not affect the P -values. Approximately 25,000 genes with zero counts in all samples (separately for the FSHD versus unaffected data and PMO data) were excluded when computing false-discovery rates.

Some remarks on DUX4. The *DUX4* gene does not itself appear as significantly differentially expressed in the RNA-seq comparison of FSHD versus unaffected myotubes (see **Supplementary Table S3**) or of FM10 versus control PMO-treated FSHD myotubes (see **Supplementary Table S2**). This is due to a combination of low expression levels and non-unique mapping: the GRCh37 reference genome has 10 annotated *DUX4* genes and pseudogenes on chromosome 4 (named *DUX4* and *DUX4L2* to *DUX4L9*, some but not all are 100% identical); it also includes six *DUX4* pseudogenes with over 99% homology on chromosome 10 (*DUX4L10* to *DUX4L15*). (Note that the Illumina iGenomes reference files do not include unplaced contig sequences; if these are included, the number of matches to reads from *DUX4* may exceed the TopHat2 default value of 20 for the “-max-multihits” option; this may also happen in the newer GRCh38 assembly.) Because htseq-count does not count multimapping reads, the *DUX4* genes usually all end up with zero counts. Inspecting the TopHat2 alignment files, there are often a smattering of reads mapping to the *DUX4* genes on chromosome 4, and these reads typically also map to between 5 and 16 other locations in the genome, depending on whether they fall in a region of perfect homology with the copies on chromosome 10, and occasionally with *DUX4* homologs on other chromosomes. The expression is low regardless of how the mapping ambiguity is resolved, however, as there were typically fewer than 10 paired-end reads out of 100 million, or 0.1 fragments per million (FPM), mapping to *DUX4* genes on chromosome 4, even for FSHD-derived myotubes. For this we used featureCounts (1.5.1) (ref. 38), with options $-M -p -O -s2$; using $-M$ but not $-fraction$ gives full (not fractional) counts for multimapping reads, so we computed the FPM from counts to a single *DUX4* gene, the copy named *DUX4L2* (ENSG00000259128) that is most telomeric on chromosome 4 in GRCh37, although in this assembly it does not include the PAS-containing exon 3. Counts for the internal copy named *DUX4* (ENSG00000258389) were nearly the same, as expected due to multimapping of the reads. Only myotubes derived from subject 17A had FPM > 0.11 for *DUX4L2*; these showed a reduction from 0.38 to 0.16 FPM in replicate 1, and from 0.25 to 0.14 FPM in replicate 2, for treatment with FM10 compared with the standard control PMO. There were no reads mapping to *DUX4* in the other samples in the PMO study (15A, 15U, or 17V).

Xenograft procedure and local delivery of PMO-ASO. The Institutional Animal Care and Use Committee at the Johns Hopkins University School of Medicine approved all procedures performed in this study. NOD-Rag1^{nu/nu}IL2r^{nu/nu} immunodeficient mice (NRG) (Stock 007799, The Jackson Laboratory, Bar Harbor, ME) were used. The xenografting procedure was performed with biceps muscle biopsies from FSHD subjects 58A, 61A, and 61B, as previously described.²² Human skeletal muscle xenografts which had fully regenerated in host NRG mice for 4–6 months were used in this study. For delivery of PMO-ASO, xenografts were first injected with 12 μl of 0.4 U/ μl bovine hyaluronidase (Sigma Aldrich, Natick, MA). Xenografts were injected with 20 μg (1 $\mu\text{g}/\mu\text{l}$) of Standard Control PMO-ASO or FM10 PMO-ASO after 2 hours. Immediately following injection, the ASO was electroporated using the parameters of 50V/cm, 10 pulses at 1 Hz, and 20 millisecond duration per pulse. Mice were euthanized 2 weeks after electroporation and human xenograft muscles were collected and snap frozen until analysis.

SUPPLEMENTARY MATERIAL

Table S1. Morpholino sequences directed at the *DUX4* transcript.

Table S2. Forty seven genes differentially expressed (with P -value $< 10^{-4}$) in FM10 versus control PMO-treated FSHD myotubes, sorted by P -value.

Table S3. One hundred and twenty five genes differentially expressed (with P -value $< 10^{-4}$) in myotubes of FSHD patients versus unaffected first degree relatives, sorted by P -value.

Table S4. Clinical characteristics of FSHD subjects and unaffected donors.

Table S5. qPCR primer sequences.

Figure S1. Effects of morpholinos on biomarker gene expression.

Figure S2. Cell toxicity assay of FM10 morpholino conjugated to Peptide B (PPMO).

Figure S3. ED₅₀ assay of FM10 PMO.

Figure S4. RNA-seq counts for five *DUX4* targets and *MYH1*, a marker of myogenic cell differentiation.

ACKNOWLEDGMENTS

This work was supported by the NIH (R21NS079529 to K.R.W. and U54HD060848 to C.P.E.). All authors contributed to the study design. N.P.C. and B.M.W. provided reagents. J.C.J.C., Y.Z., C.S., and N.P.C. conducted experiments. J.C.J.C., O.D.K., Y.Z., N.P.C., C.P.E., and K.R.W. analyzed data. J.C.J.C., Y.Z., O.D.K., C.P.E., and K.R.W. wrote the manuscript. The authors acknowledge Takako I. Jones and Peter L. Jones for *DUX4* detection methodology; Genila Bibat, Daniel Perez and the FSH Society, Inc. for assistance with patient recruitment and biopsy procurement; and Steven A. Moore and the University of Iowa Diagnostic Lab for genotyping of FSHD subjects. N.P.C. is an employee/shareholder of Sanofi Genzyme. B.M.W. is an employee/shareholder of Sarepta and of Sanofi Genzyme. Other authors have declared no conflicts of interest.

REFERENCES

- Gabriëls, J, Beckers, MC, Ding, H, De Vriese, A, Plaisance, S, van der Maarel, SM *et al.* (1999). Nucleotide sequence of the partially deleted D4Z4 locus in a patient with FSHD identifies a putative gene within each 3.3 kb element. *Gene* **236**: 25–32.
- Lemmers, RJ, Tawil, R, Petek, LM, Balog, J, Block, GJ, Santen, GW *et al.* (2012). Digenic inheritance of an SMCHD1 mutation and an FSHD-permissive D4Z4 allele causes facioscapulohumeral muscular dystrophy type 2. *Nat Genet* **44**: 1370–1374.
- de Greef, JC, Lemmers, RJ, van Engelen, BG, Sacconi, S, Venance, SL, Frants, RR *et al.* (2009). Common epigenetic changes of D4Z4 in contraction-dependent and contraction-independent FSHD. *Hum Mutat* **30**: 1449–1459.
- Lemmers, RJ, van der Vliet, PJ, Klooster, R, Sacconi, S, Camaño, P, Dauwerse, JG *et al.* (2010). A unifying genetic model for facioscapulohumeral muscular dystrophy. *Science* **329**: 1650–1653.
- Snider, L, Geng, LN, Lemmers, RJ, Kyba, M, Ware, CB, Nelson, AM *et al.* (2010). Facioscapulohumeral dystrophy: incomplete suppression of a retrotransposed gene. *PLoS Genet* **6**: e1001181.
- van Overveld, PG, Lemmers, RJ, Sandkuijl, LA, Enthoven, L, Winokur, ST, Bakels, F *et al.* (2003). Hypomethylation of D4Z4 in 4q-linked and non-4q-linked facioscapulohumeral muscular dystrophy. *Nat Genet* **35**: 315–317.
- Clapp, J, Mitchell, LM, Bolland, DJ, Fantes, J, Corcoran, AE, Scotting, PJ *et al.* (2007). Evolutionary conservation of a coding function for D4Z4, the tandem DNA repeat mutated in facioscapulohumeral muscular dystrophy. *Am J Hum Genet* **81**: 264–279.
- Tawil, R, van der Maarel, SM and Tapscott, SJ (2014). Facioscapulohumeral dystrophy: the path to consensus on pathophysiology. *Skelet Muscle* **4**: 12.

9. Geng, LN, Yao, Z, Snider, L, Fong, AP, Cech, JN, Young, JM *et al.* (2012). DUX4 activates germline genes, retroelements, and immune mediators: implications for facioscapulohumeral dystrophy. *Dev Cell* **22**: 38–51.
10. Yao, Z, Snider, L, Balog, J, Lemmers, RJ, Van Der Maarel, SM, Tawil, R *et al.* (2014). DUX4-induced gene expression is the major molecular signature in FSHD skeletal muscle. *Hum Mol Genet* **23**: 5342–5352.
11. Kowaljow, V, Marcowycz, A, Anseau, E, Conde, CB, Sauvage, S, Mattéotti, C *et al.* (2007). The DUX4 gene at the FSHD1A locus encodes a pro-apoptotic protein. *Neuromuscul Disord* **17**: 611–623.
12. Wallace, LM, Garwick, SE, Mei, W, Belayew, A, Coppee, F, Ladner, KJ *et al.* (2011). DUX4, a candidate gene for facioscapulohumeral muscular dystrophy, causes p53-dependent myopathy in vivo. *Ann Neurol* **69**: 540–552.
13. Anthony, K, Arechavala-Gomez, V, Ricotti, V, Torelli, S, Feng, L, Janghra, N *et al.* (2014). Biochemical characterization of patients with in-frame or out-of-frame DMD deletions pertinent to exon 44 or 45 skipping. *JAMA Neurol* **71**: 32–40.
14. Ionis Pharmaceuticals, I (2014-[cited Jan 24, 2016]). *A Safety and Tolerability Study of Multiple Doses of ISIS-DMPKRx in Adults With Myotonic Dystrophy Type 1*. ClinicalTrials.gov [Internet]. National Library of Medicine (US): Bethesda (MD). <http://clinicaltrials.gov/show/NCT02312011>.
15. Voit, T, Topaloglu, H, Straub, V, Muntoni, F, Deconinck, N, Campion, G *et al.* (2014). Safety and efficacy of drisapersen for the treatment of Duchenne muscular dystrophy (DEMAND II): an exploratory, randomised, placebo-controlled phase 2 study. *Lancet Neurol* **13**: 987–996.
16. Zanetta, C, Nizzardo, M, Simone, C, Monguzzi, E, Bresolin, N, Comi, GP *et al.* (2014). Molecular therapeutic strategies for spinal muscular atrophies: current and future clinical trials. *Clin Ther* **36**: 128–140.
17. <http://www.gene-tools.com>.
18. Blum, M, De Robertis, EM, Wallingford, JB and Niehrs, C (2015). Morpholinos: Antisense and Sensibility. *Dev Cell* **35**: 145–149.
19. Eisen, JS and Smith, JC (2008). Controlling morpholino experiments: don't stop making antisense. *Development* **135**: 1735–1743.
20. Marsollier, AC, Ciszewski, L, Mariot, V, Popplewell, L, Voit, T, Dickson, G *et al.* (2016). Antisense targeting of 3' end elements involved in DUX4 mRNA processing is an efficient therapeutic strategy for facioscapulohumeral dystrophy: a new gene-silencing approach. *Hum Mol Genet* **25**: 1468–1478.
21. Clayton, NP, Nelson, CA, Weeden, T, Taylor, KM, Moreland, RJ, Scheule, RK *et al.* (2014). Antisense oligonucleotide-mediated suppression of muscle glycogen synthase 1 synthesis as an approach for substrate reduction therapy of pompe disease. *Mol Ther Nucleic Acids* **3**: e206.
22. Zhang, Y, King, OD, Rahimov, F, Jones, TI, Ward, CW, Kerr, JP *et al.* (2014). Human skeletal muscle xenograft as a new preclinical model for muscle disorders. *Hum Mol Genet* **23**: 3180–3188.
23. Ferreboeuf, M, Mariot, V, Bessières, B, Vasiljevic, A, Attié-Bitach, T, Collardeau, S *et al.* (2014). DUX4 and DUX4 downstream target genes are expressed in fetal FSHD muscles. *Hum Mol Genet* **23**: 171–181.
24. Krom, YD, Dumonceaux, J, Mamchaoui, K, den Hamer, B, Mariot, V, Negroni, E *et al.* (2012). Generation of isogenic D4Z4 contracted and noncontracted immortal muscle cell clones from a mosaic patient: a cellular model for FSHD. *Am J Pathol* **181**: 1387–1401.
25. Vanderplanck, C, Anseau, E, Charron, S, Stricwant, N, Tassin, A, Laoudj-Chenivresse, D *et al.* (2011). The FSHD atrophic myotube phenotype is caused by DUX4 expression. *PLoS One* **6**: e26820.
26. Deidda, G, Cacurri, S, Piazza, N and Felicetti, L (1996). Direct detection of 4q35 rearrangements implicated in facioscapulohumeral muscular dystrophy (FSHD). *J Med Genet* **33**: 361–365.
27. Lemmers, RJ, de Kievit, P, Sandkuijl, L, Padberg, GW, van Ommen, GJ, Frants, RR *et al.* (2002). Facioscapulohumeral muscular dystrophy is uniquely associated with one of the two variants of the 4q subtelomere. *Nat Genet* **32**: 235–236.
28. van Deutekom, JC, Wijmenga, C, van Tienhoven, EA, Gruter, AM, Hewitt, JE, Padberg, GW *et al.* (1993). FSHD associated DNA rearrangements are due to deletions of integral copies of a 3.2kb tandemly repeated unit. *Hum Mol Genet* **2**: 2037–2042.
29. Wijmenga, C, Hewitt, JE, Sandkuijl, LA, Clark, LN, Wright, TJ, Dauwese, HG *et al.* (1992). Chromosome 4q DNA rearrangements associated with facioscapulohumeral muscular dystrophy. *Nat Genet* **2**: 26–30.
30. Rahimov, F, King, OD, Leung, DG, Bibat, GM, Emerson, CP Jr, Kunkel, LM *et al.* (2012). Transcriptional profiling in facioscapulohumeral muscular dystrophy to identify candidate biomarkers. *Proc Natl Acad Sci USA* **109**: 16234–16239.
31. Jones, TI, Chen, JC, Rahimov, F, Homma, S, Arashiro, P, Beermann, ML *et al.* (2012). Facioscapulohumeral muscular dystrophy family studies of DUX4 expression: evidence for disease modifiers and a quantitative model of pathogenesis. *Hum Mol Genet* **21**: 4419–4430.
32. Homma, S, Chen, JC, Rahimov, F, Beermann, ML, Hanger, K, Bibat, GM *et al.* (2012). A unique library of myogenic cells from facioscapulohumeral muscular dystrophy subjects and unaffected relatives: family, disease and cell function. *Eur J Hum Genet* **20**: 404–410.
33. Jones, TI, King, OD, Himeda, CL, Homma, S, Chen, JC, Beermann, ML *et al.* (2015). Individual epigenetic status of the pathogenic D4Z4 macrosatellite correlates with disease in facioscapulohumeral muscular dystrophy. *Clin Epigenetics* **7**: 37.
34. Kim, D, Perte, G, Trapnell, C, Pimentel, H, Kelley, R and Salzberg, SL (2013). TopHat2: accurate alignment of transcriptomes in the presence of insertions, deletions and gene fusions. *Genome Biol* **14**: R36.
35. Langmead, B and Salzberg, SL (2012). Fast gapped-read alignment with Bowtie 2. *Nat Methods* **9**: 357–359.
36. Anders, S, Pyl, PT and Huber, W (2015). HTSeq—a Python framework to work with high-throughput sequencing data. *Bioinformatics* **31**: 166–169.
37. McCarthy, DJ, Chen, Y and Smyth, GK (2012). Differential expression analysis of multifactor RNA-Seq experiments with respect to biological variation. *Nucleic Acids Res* **40**: 4288–4297.
38. Liao, Y, Smyth, GK and Shi, W (2014). Feature Counts: an efficient general purpose program for assigning sequence reads to genomic features. *Bioinformatics* **30**: 923–930.



This work is licensed under a Creative Commons Attribution-NonCommercial-ShareAlike 4.0 International License. The images or other third party material in this article are included in the article's Creative Commons license, unless indicated otherwise in the credit line; if the material is not included under the Creative Commons license, users will need to obtain permission from the license holder to reproduce the material. To view a copy of this license, visit <http://creativecommons.org/licenses/by-nc-sa/4.0/>

© J CJ Chen *et al.* (2016)